

Article

Bulk Viscous Flat FLRW Model with Observational Constraints in $f(T, B)$ Gravity

Archana Dixit¹ and Anirudh Pradhan^{2,*} 

¹ Department of Mathematics, Institute of Applied Sciences and Humanities, GLA University, Mathura 281406, Uttar Pradesh, India

² Centre for Cosmology, Astrophysics and Space Science (CCASS) GLA University, Mathura 281406, Uttar Pradesh, India

* Correspondence: pradhan.anirudh@gmail.com

Abstract: This paper investigates the impact of bulk viscosity within the framework of $f(T, B)$ gravity. We consider a time-dependent viscosity model with a particular Hubble parameter expression. Here, we looked into the viability of well-motivated $f(T, B)$ gravity model, which takes the form $f = \alpha \log(B) + \beta T$, and has free parameters α and β . The 46 observational Hubble data (OHD) in the range $0 \leq z \leq 2.36$ were used to constrain the model parameters to achieve the solution. We have used the Markov Chain Monte Carlo (MCMC) method to estimate model parameters and observe that the model appears to be in good agreement with the observations. In addition, we evaluate the effective viscous equation of state parameter for the $f(T, B)$ model. We have examined the characteristics of different energy conditions for the stability analysis. The model is valid based on the positive behavior of null energy conditions (NEC), weak energy conditions (WEC), and dominant energy conditions (DEC); however, strong energy conditions (SEC) are in violation, suggesting that the universe is expanding faster. Our model was found in the quintom region. We also discussed how the tachyon scalar field corresponds to $f(T, B)$ gravity.

Keywords: modified gravity; cosmology; $f(T, B)$ gravity; viscosity

PACS: J04.50.-h; 98.80.-k; 65.40.gd



Citation: Dixit, A.; Pradhan, A. Bulk Viscous Flat FLRW Model with Observational Constraints in $f(T, B)$ Gravity. *Universe* **2022**, *8*, 650. <https://doi.org/10.3390/universe8120650>

Academic Editor: Lorenzo Iorio

Received: 26 October 2022

Accepted: 29 November 2022

Published: 7 December 2022

Publisher's Note: MDPI stays neutral with regard to jurisdictional claims in published maps and institutional affiliations.



Copyright: © 2022 by the authors. Licensee MDPI, Basel, Switzerland. This article is an open access article distributed under the terms and conditions of the Creative Commons Attribution (CC BY) license (<https://creativecommons.org/licenses/by/4.0/>).

1. Introduction

Mathematical and theoretical aspects of cosmic physics have changed as a result of the cosmic microwave background radiation (CMBR), observations of supernovae of type Ia, and other discoveries; see references [1–4] for more information. As we know, the field of cosmology has given conclusive proof that the universe is expanding. Gravitational theories consistent with observations play a significant role in explaining the universe's origin and the presence of relativistic star populations. The most prominent method for studying cosmic acceleration is the exposure of modified gravitational theories (MGTs) developed by modifying the Einstein–Hilbert (EH) action. Geometric constants, which modify the gravitational field equations, can be used to generate modified theories of gravity using the Einstein–Hilbert action [5,6]. This adds new dynamical degrees of freedom to the field equations, driving the dynamics and illuminating the observed phenomena [7–12].

In general relativity (GR), the Ricci scalar R of the Levi–Civita symmetric connection is the fundamental invariant. However, this is not the case in the Teleparallel Equivalent of General Relativity (TEGR), where the gravitational is determined by using the fundamental geometric invariant. The torsion scalar T is part of the action integral. It is defined by the antisymmetric connection of the non-holonomic basis, which is called the curvature-less Weitzenböck connection [13,14]. In literature, there are various modified theories influenced by teleparallelism that have yielded a variety of intriguing findings in cosmology and astrophysics [15,16] like $f(R)$ theory [8,17,18], $f(T)$ theory [19–22], $f(T, B)$ theory [23–25],

$f(R, T)$ theory [26–31], $f(Q, T)$ theory [32,33], $f(G)$ theory [34], $f(R, G)$ theory [35], $f(Q)$ theory [18,36–38], $F(R, T, Q, \tau)$ theory [39], etc. Recently, Mardan et al. [40] have investigated the conformally flat spherically symmetric fluid distribution with a generalized polytropic equation of state in $f(R)$ gravity. Noureen et al. [41] also developed a general framework to observe the instabilities in self-gravitating spherically symmetric through cracking with anisotropic inner matter configuration in $f(R)$ gravity. The impact of $f(R, T)$ gravity in the evolution of charged viscous fluids is studied by Noureen et al. [42].

These days, The $f(T, B)$ theory of gravity has been thoroughly investigated. We are interested in the $f(T, B)$ theory, also known as the fourth-order teleparallel theory of gravity. The gravitational action integral is defined by an arbitrary function f of the torsion scalar T and the boundary term B , which is related to the torsion scalar and the Ricci scalar, $B = R + T$ [43,44]. Shekh et al. [45] have recently investigated the physical acceptability of FLRW universe filled with two fluids, first the pressureless matter and the second as different types of holographic dark energy in $f(T, B)$ gravity. The cosmography for high redshifts in $f(T, B)$ gravity has been discussed by Escamilla-Rivera et al. [46] through the statistical performance of cosmological observations. In the present day, the generalization of the teleparallel theory has gained significant importance, which could provide alternative explanations for the acceleration of the cosmos. The fact that the invariance under local Lorentz transformations is broken is one of the most significant issues with the $f(T)$ theory of gravity. If there is no local Lorentz symmetry, then there is no way to fix any of the four components that make up the tetrad [47]. As we know, if the Lorentz invariance is lost, two different tetrads that have the same metric could give different field equations. In reference [48], a new method was used to develop a new way to build a covariant formulation of $f(T)$ gravity. The authors [23] introduce new $f(T)$ gravity, which is more general, by adding a new Lagrangian function $f(T, B)$, which has a boundary term B that is related to the divergence of the torsion tensor. If we select the special form of $f(-T + B)$, this theory is the same as $f(R)$ gravity.

In cosmology, several investigations have been done in the framework of $f(T, B)$ -gravity. In the literature [49–54], many cosmologist have discussed the exact and analytical cosmological solutions with an isotropic background, which are focused on the reconstruction of the cosmic history in the $f(T, B)$ theory. The presence of nonzero spatial curvature was recently considered in [55]. A new inhomogeneous precise solution was discovered in [56], whereas [57] examined the minisuperspace quantization in $f(T, B)$. The analysis of anisotropic solution in $f(T, B)$ is the most recent research, which is discussed in [44]. They observed that Kasner and Kasner-like solutions are asymptotic solutions for the field equations; however, the theory does not favor anisotropic exponential solutions.

In this context, bulk viscosity is an important part of cosmology for studying how the universe has changed over time because it tells us many interesting phenomena about how homogeneous cosmological models work. The measurement of a fluid's resistance to flow is referred to as its viscosity. Viscosities can be divided into two categories: bulk viscosity and shear viscosity. Most of the time, bulk viscosity is related to an isotropic universe, while shear viscosity is related to an anisotropic universe. Bulk viscosity plays an important role in cosmic expansion and pressure. The concept of viscous dark energy (DE) models has been given in several ways to understand the development of the cosmos. Ren and Meng [58] examined the development of the cosmos using a cosmological model with bulk viscosity. Tawfik and Harko [59] investigated the phase transition of the viscous early universe. The concept of bulk viscosity has also been thoroughly researched in modified gravity. Sharif and Rani [60] studied bulk viscosity in $f(T)$ theory, where " T is the torsion scalar". In this theory, the authors [61] investigated viscous and non-viscous holographic DE models. In this paper, we investigate the cosmological implications of the $f(T, B)$ gravity model with viscous fluid. This paper focuses on the effect of fluid viscosity in the $f(T, B)$ -gravity model.

The manuscript is organized as follows: we have discussed the basic formalism of $f(T, B)$ gravity in Section 2. The cosmological model with observational constraint is discussed in Section 3. Dynamical parameters and their physical discussion for viscous

fluid are mentioned in Section 4. The energy conditions are discussed in Section 5. We have discussed the $f(T, B)$ tachyon model in Section 6. Conclusions are mentioned in Section 7.

2. Basic Formalism of $f(T, B)$ Gravity

The fundamental formalism of $f(T, B)$ gravity and its field equations [44,62] are introduced in this section. For the combination of $f(T)$ and $f(R)$ gravity, take into account the following action, which is $f(T, B)$ gravity [63] as

$$S = \int e \left(\frac{f(T, B)}{\kappa^2} + L_m \right) d^4x, \tag{1}$$

where $\kappa^2 = 8\pi G$ and $f(T, B)$ are a function of the torsion scalar T and the boundary term $B = \frac{2}{e} \partial_\mu (e T^\mu)$ in which $T_\mu = T^\mu_{\nu}$. Here, L_m and $e = \det(e^i_\mu)$ are the tetrad component's matter action and determinant, respectively. The field equation can be defined by varying the action given in Equation (1) with respect to the tetrad.

$$2\delta^\lambda_\nu \nabla^\mu \nabla_\mu e f_B - 2e \nabla^\lambda \nabla_\nu f_B + B f_B \delta^\lambda_\nu + 4e [\partial_\mu e f_B + \partial_\mu f_T] S_\nu^{\lambda\mu} + 4e^\alpha_\nu \partial_\mu (e S^\mu_\alpha \lambda) f_T - 4e f_T T^\alpha_{\mu\nu} S^{\lambda\mu} - e f \delta^\lambda_\nu = 16\pi e \tau^\lambda_\nu, \tag{2}$$

where $\tau^\lambda_\nu = a^\alpha_\nu T^\lambda_\alpha$ is the standard energy momentum tensor and $\square = \Delta^\mu \Delta_\mu$. This work aims to establish several well-motivated $f(T, B)$ gravity models and confine them to flat FRW spacetime. The following metric describes this space-time in cartesian coordinates:

$$ds^2 = -dt^2 + a(t)^2(dx^2 + dy^2 + dz^2); \tag{3}$$

where $a(t)$ represents the scale factor of the universe. In these coordinates, the tetrad field can be expressed as follows [64]:

$$e^a_\mu = \text{diag}(1, a(t), a(t), a(t)). \tag{4}$$

The explicit torsion scalar for this spacetime is provided by

$$T = 6H^2. \tag{5}$$

In contrast, the boundary term is provided by

$$B = (6\dot{H} + 18H^2). \tag{6}$$

The Ricci scalar and the torsion scalar are connected as

$$R = -T + B = (6\dot{H} + 12H^2). \tag{7}$$

This shows how the concept of $f(R)$ gravity is a subset of $f(T, B)$ gravity, where

$$f(T, B) = f(-T + B) = f(R), \tag{8}$$

which is only a tiny part of the models that can be made in $f(T, B)$ gravity. In addition, the contributions of the torsion scalar and the boundary term, which are of the second and fourth orders, respectively, can be viewed simply through the utilization of this particular tetrad. When the field equations for a universe, that is filled with a perfect fluid, are evaluated, the Friedmann result comes out [23,65] as:

$$-3H^2(3f_B + 2f_T) + 3\dot{H} + \dot{f}_B - 3\dot{H}f_B + \frac{1}{2}F = \kappa^2 \rho, \tag{9}$$

$$-(3H^2 + \dot{H})(3f_B + 2f_T) - 2H\dot{f}_T + \ddot{f}_B + \frac{1}{2}f = -\kappa^2 p, \tag{10}$$

where ρ and p are, respectively, the energy density and pressure of the perfect fluid. The Friedmann equations show how a linear boundary contribution to the Lagrangian might function as a boundary term in Equations (9) and (10). Other contributions of B would nontrivially alter the dynamics of these equations at the same time.

Bulk Viscosity

The bulk viscosity in $f(T, B)$ gravity is described in this section. Another way to define bulk viscosity is to change the pressure (p) term by adding a dissipative term, Π , so that the effective pressure p_{eff} is given by [66]:

$$p_{eff} = p + \Pi. \tag{11}$$

Eckart [67] introduced the effective pressure in thermodynamical systems for relativistic dissipative processes, where Π signifies the dissipative process and equals $-3H\zeta(t)$. The bulk viscosity function is $\zeta(t)$ here. Since bulk viscosity of the fluid was assumed, the energy-momentum tensor with the viscous term is defined [66] as follows:

$$T^i_j = (\rho + p_{eff})u^j u_i - p_{eff}\delta^i_j. \tag{12}$$

The four-velocity is $u^k = (1, 0, 0, 0)$ and $\delta^i_j = 1$ for $i = j$ and $\delta^i_j = 0$ for $i \neq j$. As we know, the shear viscosity does not contribute to the energy-momentum tensor in the background of the FRW metric, but bulk viscosity appears as an effective pressure. By considering $p_m = 0$, the field Equations (9) and (10) can be written as:

$$3H^2 = \kappa^2(\rho_m + \rho_T), \tag{13}$$

$$3H^2 + 2\dot{H} = -\kappa^2 p_T, \tag{14}$$

where the modified TEGR components are present in the effective fluid contributions as

$$3H^2(1 + 3f_B + 2f_T) + 3\dot{H} + \dot{f}_B - 3\dot{H}f_B - \frac{1}{2}f = \kappa^2 \rho_T, \tag{15}$$

$$-3H^2(1 + 3f_B + 2f_T) - \dot{H}(2 + 3\dot{f}_B + 2\dot{f}_T) - 2H\dot{f}_T + \ddot{f}_B + \frac{1}{2}f = \kappa^2 p_T, \tag{16}$$

where $\dot{f}_T = f_{TT}\dot{T} + f_{TB}\dot{B}$, $\dot{f}_B = f_{TB}\dot{T} + f_{BB}\dot{B}$ and $\ddot{f}_B = f_{TTB}\dot{T}^2 + 2f_{TBB}\dot{T}\dot{B} + f_{BBB}\dot{B}^2 + f_{TB}\ddot{T} + f_{BB}\ddot{B}$, these are denote the multiple partial derivation with respect to T and B . The ρ_T and p_T are the components of the effective energy density and effective pressure, respectively, from $f(T, B)$ gravity, and these are representative of DE. The expressions of ρ_T and p_T that are shown in Equations (15) and (16) are slightly different from those that are shown in equations Equations (9) and (10) because the standard Friedmann equations are shown in Equations (13) and (14). As a result, we conclude that Equations (15) and (16) represent the density and pressure of dark energy for the $f(T, B)$ gravity model. For the purpose of discussion, we have assumed that the $f(T, B)$ gravity model of the form $f(T, B) = \gamma \log(B) + \beta T$, where $\gamma \neq 0$ and $\beta \neq 0$. The equation of state (EoS) parameter of a perfect fluid is proportional to the ratio of its pressure and density, whereas the EoS parameter of a viscous fluid is denoted by

$$\omega_{eff} = \frac{p_T + 3H\zeta}{\rho_m + \rho_T}. \tag{17}$$

The EoS parameter is an essential parameter of the universe. As we know, the equation of the state parameter is associated with energy density and pressure, which classifies the universe’s expansion. In the de Sitter universe, $\dot{H} = 0$, we have $\omega_T = -1$, which behaves similarly to the cosmological constant.

3. Cosmological Model with Observational Constraints

A Hubble parameter H must be utilized to obtain an expanding universe model that agrees with observations. This model must start out decelerating and then accelerate through time. As a one-parameter function discussed in [68], we look into the variation of the Hubble parameter H .

$$H(a) = \alpha(a^{-m} - 1), \tag{18}$$

where $\alpha > 0$ and $(m > 1)$ both are constants in the expression. The value of q for the deceleration parameter is obtained as

$$q = \frac{m}{a^m + 1} - 1. \tag{19}$$

In the context of Robertson–Walker space-time, Banerjee and Das [69] also proposed a similar form of q . When $a = 0$, $q = m - 1$, $q = 0$ for $a^m = m - 1$, and for $a^m > m - 1$, $q < 0$, we can see from (19). For $t = 0$, we assume that $a = 0$. As a result, the universe starts from the decelerating phase and then transitions to an accelerating one. This cosmological scenario provides a unified view of the expansion history of the evolving universe and is consistent with SNe Ia astronomical observations [1,70]. By using Equations (18) and (19), we obtained H as

$$H^{-1} = -\frac{1 + q - m}{m a} \tag{20}$$

Integrating Equation (18), we obtain

$$a^m = e^{-1+ma(t+k_1)}, \tag{21}$$

where k_1 is a constant of integration. Assuming $a = 0$ for $t = 0$, we obtain $k_1 = 0$. Therefore,

$$a = (e^{mat-1})^{1/m}. \tag{22}$$

The scale factor (a) and the redshift (z) [71–73] are related in the following way:

$$a = \frac{a_0}{(1 + z)} \tag{23}$$

As a result, the Hubble parameter for the redshift is as follows:

$$H(z) = \frac{H_0}{2} [1 + (1 + z)^m], \tag{24}$$

where H_0 presents the value of the Hubble parameter [74]. One of the most significant quantities in cosmology is the Hubble constant because it tells us how fast the universe is expanding, which may be used to calculate the age and history of the universe. The Hubble constant is defined as the unit of measurement, which is used for describing the expansion of the universe. Hubble’s constant H is 160 km/s per million-light-years. In astrophysics, gravitational redshift is denoted by a dimensionless quantity z (which is a function of the radius of compact star r) and is defined as follows: $1 + z(r) = \text{Observed wavelength}/\text{Actual wavelength}$, as such when $z > 0$, it exhibits a redshift effect, otherwise it is a blueshift. In a special case, a gravitational redshift is considered as a surface redshift at the surface of the star, i.e., $r = R$ and hence one obtains $z_g = z_s (r = R)$. In essence, a surface redshift of a star is then implying that it is nothing but a gravitational redshift on the surface only, however the redshift will now be dependent on the mass or more precisely density of the star, what is generally known as the surface gravity. As such, in the case of an astrophysical object, a gravitational redshift will be maximum on the surface and minimum at the center of a compact star. In this section, we present the observational data and statistical methodology used to constrain the model parameters of the derived universe (see Figures 1 and 2). Here, we applied 46 $H(z)$ observational data points ranges $0 \leq z \leq 2.36$ see Table 1, which were

obtained by using the Markov Chain Monte Carlo (MCMC) method. To determine the best-fitting values and limits for a fitted model, we use the χ^2 statistic [75,76]. According to 46 observational Hubble data (OHD), the estimated values of are $H_0 = 65 \pm 0.12 \text{ kms}^{-1} \text{ Mpc}^{-1}$ and $m = 1.5^{+0.0026}_{-0.0026}$. To limit the model's parameters H_0 and m , we defined χ^2 as

$$\chi^2(H_0, m) = \sum_{i=1}^{46} \frac{(H_{th}(i) - H_{ob}(i))^2}{\sigma(i)^2} \tag{25}$$

where $H_{th}(i)$ denotes the theoretical values of $H(z)$ according to [23], and $\sigma(i)$'s denotes errors in the observed values of $H(z)$ ". In Figure 1, the 1-dimensional marginalized distribution and 2-dimensional contours were obtained for our derived model with 68.3%, 95.4%, and 99.7% confidence levels, respectively.

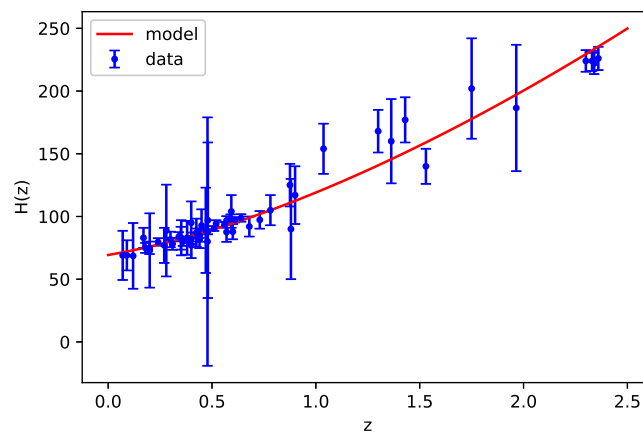


Figure 1. Error bar plot of $H(z)$ versus redshift z .

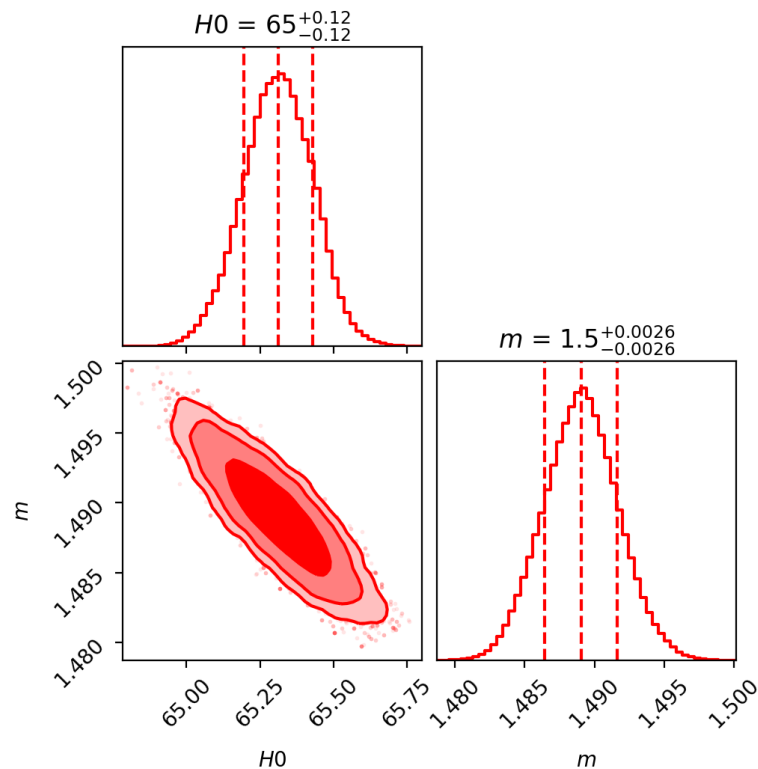


Figure 2. One-dimensional and two-dimensional marginalized confidence regions (68%CL and 95% CL) for a, H_0 obtained from the 46 OHD data for the $f(T, B)$ gravity model.

Table 1. The behavior of Hubble parameter $H(z)$ with redshift.

S.No	Z	H(Obs)	σ_i	Reference	S.No	Z	H(Obs)	σ_i	Reference
1	0	67.77	1.30	[77]	24	0.4783	80.9	9	[78]
2	0.07	69	19.6	[79]	25	0.48	97	60	[80]
3	0.09	69	12	[81]	26	0.51	90.4	1.9	[82]
4	0.01	69	12	[80]	27	0.57	96.8	3.4	[83]
5	0.12	68.6	26.2	[79]	28	0.593	104	13	[84]
6	0.17	83	8	[80]	29	0.60	87.9	6.1	[85]
7	0.179	75	4	[84]	30	0.61	97.3	2.1	[82]
8	0.1993	75	5	[84]	31	0.68	92	8	[84]
9	0.2	72.9	29.6	[79]	32	0.73	97.3	7	[85]
10	0.24	79.7	2.7	[86]	33	0.781	105	12	[84]
11	0.27	77	14	[80]	34	0.875	125	17	[84]
12	0.28	88.8	36.6	[79]	35	0.88	90	40	[80]
13	0.35	82.7	8.4	[87]	36	0.9	117	23	[80]
14	0.352	83	14	[84]	37	1.037	154	20	[84]
15	0.38	81.5	1.9	[82]	38	1.3	168	17	[80]
16	0.3802	83	13.5	[78]	39	1.363	160	33.6	[88]
17	0.4	95	17	[81]	40	1.43	177	18	[80]
18	0.4004	77	10.2	[78]	41	1.53	140	14	[80]
19	0.4247	87.1	11.2	[78]	42	1.75	202	40	[80]
20	0.43	86.5	3.7	[86]	43	1.965	186.5	50.4	[88]
21	0.44	82.6	7.8	[85]	44	2.3	224	8	[89]
22	0.44497	92.8	12.9	[78]	45	2.34	222	7	[90]
23	0.47	89	49.6	[91]	46	2.36	226	8	[92]

4. Dynamical Parameters and Their Physical Discussion for Viscous Fluid

Many authors have considered different types of bulk viscous coefficients when analyzing the various cosmological models. The features of DE are examined in this article by accounting for the bulk viscosity coefficient with pressureless fluid [93–95] as

$$\zeta = \zeta_0 + \zeta_1 H + \zeta_2 (\dot{H} + H^2) \tag{26}$$

where ζ_0 , ζ_1 , and ζ_2 are all positive coefficients.

The choice of this bulk viscosity is motivated by the fact that the phenomenon of viscosity is connected to the concepts of velocity and acceleration. We know that the specific form of viscosity cannot be determined. Here, we use a parameterized bulk viscosity, a linear combination of three factors, to discuss cosmological issues. The third term links bulk viscosity to the accelerated expansion of the universe, while the second term defines bulk viscosity proportionate to the Hubble parameter H . As a result, it is possible that the results of the linear combination of these two with the acceleration term (\ddot{a}) will be improved and yields a better result. Here, we consider the Hubble parameter, which is defined in [96] to investigate the behavior of the effective EoS parameter (ω_{eff}) as follows:

$$H = \frac{me^{amt-1}}{(e^{amt}-1)^{1/m}} \tag{27}$$

Now, solving Equations (15) and (16) with the help of Equation (27), we obtained the density and pressure of $f(T, B)$ gravity as

$$\begin{aligned} \rho_T = & \left[\frac{1}{2(e^{amt}-1)^2(m-3e^{amt})^2} \left(2\gamma m^2 + 9(6\alpha^2(\beta+1) + \gamma)e^{4amt} - 3\gamma(m+4)me^{amt} \right. \right. \\ & + 3e^{2amt} (3\gamma + 2\alpha^2(\beta+1)m^2 + 8\gamma m) + e^{3amt} (-18\gamma + \gamma m^2 - 12m(3\alpha^2(\beta+1) + \gamma)) \\ & \left. \left. - (e^{amt}-1)^2(m-3e^{amt})^2 \gamma \log \left(\frac{6\alpha^2 e^{amt} (3e^{amt}-m)}{(e^{amt}-1)^2} \right) \right) \right] \tag{28} \end{aligned}$$

$$\begin{aligned}
 p_T = & \left[\frac{e^{\alpha(-m)t}}{6(e^{\alpha mt} - 1)^2(3e^{\alpha mt} - m)^3} \left(\gamma m^4 - 2\gamma(m + 3)m^3 e^{\alpha mt} - 81(6\alpha^2(\beta + 1) + \gamma)e^{6\alpha mt} \right. \right. \\
 & + (m^3 - 6m^2 + 27m(10\alpha(\beta + 1) + 1) + 54)e^{5\alpha mt} - m^2(2m^2(6\alpha(\beta + 1) - 1) - 6m - 9)e^{2\alpha mt} \\
 & + m^2 e^{2\alpha mt} (9\gamma - 2m^2(6\alpha^2(\beta + 1) - \gamma) + 6\gamma m) + e^{4\alpha mt} (-9m^2(54\alpha^2(\beta + 1) - 5\gamma) \\
 & - 81\gamma + \gamma m^4 - 12\gamma m^3 - 162\gamma m) + 3e^{5\alpha mt} (54\gamma + \gamma m^3 - 6\gamma m^2 + 27n(10\alpha^2(\beta + 1) + \gamma)) \\
 & + m e^{3\alpha mt} (81\gamma - 2\gamma m^3 + 9m^2(14\alpha^2(\beta + 1) + \gamma) - 36\gamma m) \\
 & \left. \left. + 3\gamma e^{\alpha mt} (e^{\alpha mt} - 1)^2 (3e^{\alpha mt} - m)^3 \log \left(\frac{6\alpha^2 e^{\alpha mt} (3e^{\alpha mt} - m)}{(e^{\alpha mt} - 1)^2} \right) \right) \right] \tag{29}
 \end{aligned}$$

Now, solving Equations (28) and (29), we obtained the EoS parameter of $f(T, B)$ gravity as:

$$\begin{aligned}
 \omega_{peff} = & \left[\frac{\alpha^2 e^{2\alpha mt}}{18(e^{\alpha mt} - 1)^2} \left(- \frac{18\alpha e^{\alpha mt} (a(e^{\alpha mt} - 1)^2 + \alpha e^{\alpha mt} (b(e^{\alpha mt} - 1) + \alpha c(e^{\alpha mt} - m)))}{(e^{\alpha mt} - 1)^3} + \right. \right. \\
 & + \frac{18\alpha^2 \beta e^{2\alpha mt}}{(e^{\alpha mt} - 1)^2} + \frac{2\gamma m^2 e^{\alpha(-m)t} ((m - 6)e^{\alpha mt} + m)^2}{(3e^{\alpha mt} - m)^3} \\
 & + \frac{\gamma m^2 e^{\alpha(-m)t} ((m - 6)e^{2\alpha mt} + 4(m - 3)e^{\alpha mt} + m)}{(m - 3e^{\alpha mt})^2} \\
 & + \frac{3m(\gamma + (12\alpha^2(\beta + 1) + \gamma)e^{2\alpha mt} - 2e^{\alpha mt}(\gamma + 2\alpha^2(\beta + 1)m))}{(e^{\alpha mt} - 1)^2(3e^{\alpha mt} - m)} \\
 & - \frac{9e^{\alpha mt}(\gamma + (6\alpha^2(2\beta + 1) + \gamma)e^{2\alpha mt} - 2e^{\alpha mt}(\gamma + \alpha^2(2\beta + 1)m))}{(e^{\alpha mt} - 1)^2(3e^{\alpha mt} - m)} \\
 & \left. \left. + 3\gamma \log \left(\frac{6\alpha^2 e^{\alpha mt} (3e^{\alpha mt} - m)}{(e^{\alpha mt} - 1)^2} \right) \right) \right]. \tag{30}
 \end{aligned}$$

We have investigated the behavior of the EoS parameter (ω_T) with cosmic time t for the limiting conditions of the viscosity parameters shown in Figure 3a,b. The EoS parameter appears to be negative in the beginning. Consequently, it moves from the negative region to the positive region. It has been observed that ω_T has entered the positive region over time. The negative ω_T is proposed as a constant vacuum energy density. It's worth noting that $\omega_T = 0$ shows Pressureless Cold Matter (PCM), $\omega_T = 0, \frac{1}{3}$ represents Hot Matter, $\omega_T = (\frac{1}{3})$ is radiation, $\omega_T = (\frac{1}{3}, 1)$ is Hard Universe, $\omega_T = 1$ shows stiff fluid (SF), $\omega_T > 1$ is Ekpyrotic Matter (Ek-M), $\omega_T > -1$ stand for the Quintessence (Q) region and $\omega_T < -1$ stands for the Phantom (Ph) region, respectively. While $\omega_T = -1$ represents the cosmological constant (Λ CDM) and $\omega_T \ll -1$ is precluded by SN Ia perceptions (Supernovae Heritage Study, Gold example of Hubble Space Telescope) (see all details in Table 2). Subsequently, our derived model's evolving range of ω_T is supportive of the quintom region. In our derived model, the effective EoS parameter lies in the phantom region $-1 < \omega_T < -\frac{1}{3}$, crosses the cosmological constant and entered the quintences region for all the limiting conditions [97] for the viscosity parameter, see Figure 3a. Similarly, Figure 3b lies in the phantom region if $\zeta_0 < 0$ is mentioned in Table 3. The effective EoS parameter is sensitive to the choice of parameter ζ_0, ζ_1 and ζ_2 , at least at cosmic times spanning from the recent past to a late epoch. However, the presence of viscous co-efficient strongly affects the early time of evolution.

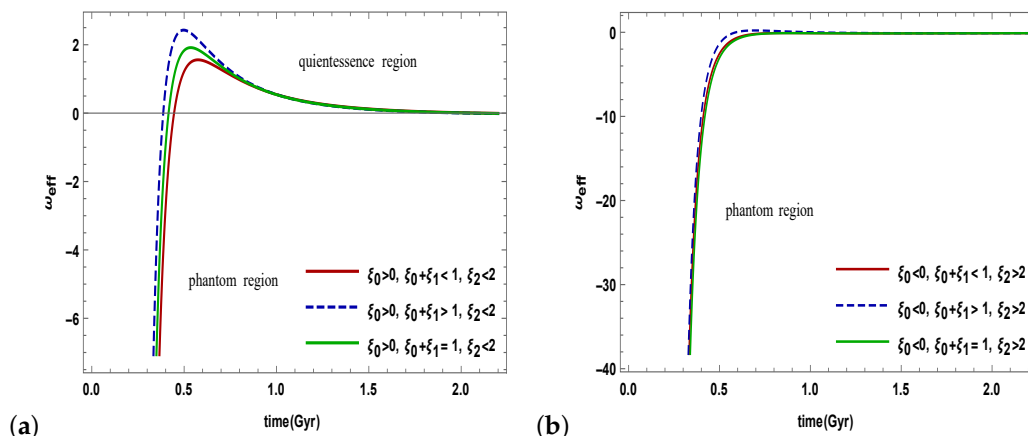


Figure 3. The variation of EoS parameter versus time t for various limiting conditions of the bulk viscosity coefficients. (a) $\zeta_0 > 0$; (b) $\zeta_0 < 0$.

Table 2. Existence of different substances according to EoS parameter.

Substance	Observation	EoS Parameter
Phantom Universe (Ph)	Lead to Big Rip, resist to weak energy condition	$\omega < -1$
Quintessence (Q)	68% of the universe	$\omega_T \in (-1/3, -1)$
Cosmological constant	Inconsistent with observation	$\omega_T = -1$
Hard Universe (HU)	high densities	$\omega_T \in (1/3, 1)$
Radiation (R)	Influential in past	$\omega_T = 1$
Hot matter (HM)	insignificant in present time	$\omega_T = 0, 1/3$
Ekyrotic matter (Ek-M)	Resist DEC	$\omega_T > 1$
Pressless cold matter (PCM)	32% of the Universe	$\omega_T = 0$
Stiff Fluid (SF)		$\omega_T = 1$

Table 3. The cosmological evolution and behavior of EoS parameter for the limiting case of ζ .

Range of ζ	ζ_0	ζ_1	ζ_2	ω_{eff}	Behavior
$\zeta_0 > 0, \zeta_0 + \zeta_1 < 1, \zeta_2 < 2$	0.9	0.02	1.5	$-8.8 \leq \omega_{eff} = 0$	Ph- Λ CDM-Ek-M- SF- PCM
$\zeta_0 > 0, \zeta_0 + \zeta_1 > 1, \zeta_2 < 2$	0.45	0.65	1.5	$-8.6 \leq \omega_{eff} = 0$	Ph- Λ CDM-Ek-M- SF- PCM
$\zeta_0 > 0, \zeta_0 + \zeta_1 = 1, \zeta_2 < 2$	0.65	0.35	1.5	$-8.5 \leq \omega_{eff} = 0$	Ph- Λ CDM-Ek-M- SF- PCM
$\zeta_0 > 0, \zeta_0 + \zeta_1 = 1, \zeta_2 > 2$	-0.5	1.45	2.1	$-37.9 \leq \omega_{eff} = 0$	Ph- Λ CDM-Ek-M- SF- PCM
$\zeta_0 < 0, \zeta_0 + \zeta_1 > 1, \zeta_2 > 2$	-0.5	2.5	3	$-37.3 \leq \omega_{eff} = 0$	Ph- Λ CDM- PCM
$\zeta_0 < 0, \zeta_0 + \zeta_1 > 1, \zeta_2 > 2$	-0.5	1.5	2.17	$-38.8 \leq \omega_{eff} = 0$	Ph- Λ CDM- PCM

5. Energy Condition

Energy conditions that assign the basic causal and geodesic structure of space-time should be put up against any alternative theory of gravity. The earliest energy conditions that were described in the literature are point-wise in nature; they limit the stress tensor’s ability to compress at every point in space. The four main conditions are the weak energy condition (WEC), the strong energy condition (SEC), the dominant energy condition (DEC) and the null energy condition (NEC).

In its physical form, the WEC requires that for every future-pointing timelike vector t^a ,

$$T_{ab}t^at^b \geq 0.$$

The SEC imposes a bound on an expression,

$$\left(T_{ab} - \frac{T}{n-2}g_{ab}\right)t^at^b \geq 0,$$

where we assume $n > 2$. The SEC is generally violated more easily than the WEC.

The physical form of the DEC can be written as

$$T_{ab}t^a\zeta^b \geq 0,$$

for any two co-oriented time-like vectors t^a and ζ^b . The DEC requires that the flux of energy-momentum measured by an observer is causal and in the direction of observer’s proper time.

The NEC is a variation of WEC, with the time-like vector replaced by a null vector k^a

$$T_{ab}k^ak^a \geq$$

The NEC is the weakest of the four main point-wise energy conditions. Please consult the references [98–100] for more information on the distinction between these energy conditions and physical importance.

Energy conditions have a great utility in classical GR which discusses the singularity problems of space-time and explain the behavior of null, space-like, time-like, or light-like geodesics [101,102]. The origin of these energy conditions is independent of any theory of gravity and is purely geometrical in nature. These circumstances guarantee the application of the second law of thermodynamics, which states that as the universe expands more quickly, energy density reduces. The universe’s quickening expansion is also known as violation (SEC). The various energy states can often be explained using the following form:

- Null energy condition (NEC) if $\rho_{eff}(t) + p_{eff}(t) \geq 0$;
- Weak energy conditions (WEC) if $\rho_{eff}(t) \geq 0, \rho_{eff}(t) + p_{eff}(t) \geq 0$;
- Strong energy conditions (SEC) if $\rho_{eff}(t) + 3p_{eff}(t) \geq 0, \rho_{eff}(t) + p_{eff}(t) \geq 0$;
- Dominant energy conditions (DEC) if $\rho_{eff}(t) \geq 0, \rho_{eff}(t) \pm p_{eff}(t) \geq 0$.

Figure 4 portrays the behavior of energy density versus time with the appropriate choice of viscous parameters as ζ . Among all the energy conditions, the strong energy condition is in the limelight of discussion. According to the recent data on the accelerating Universe, the SEC must be violated on a cosmological scale [98]. The slight change in the values of ζ towards the negative side results in the SEC’s change. SEC violates more in the range mentioned above. We can notice this in Figure 4a,c,e for the limiting conditions of the viscosity parameter $\zeta_0 > 0$ NEC, WEC, and DEC do not violate, but SEC violates. Similarly, in Figure 4b,d,f, for $\zeta_0 < 0$, NEC is satisfied, but DEC and SEC are not satisfied.

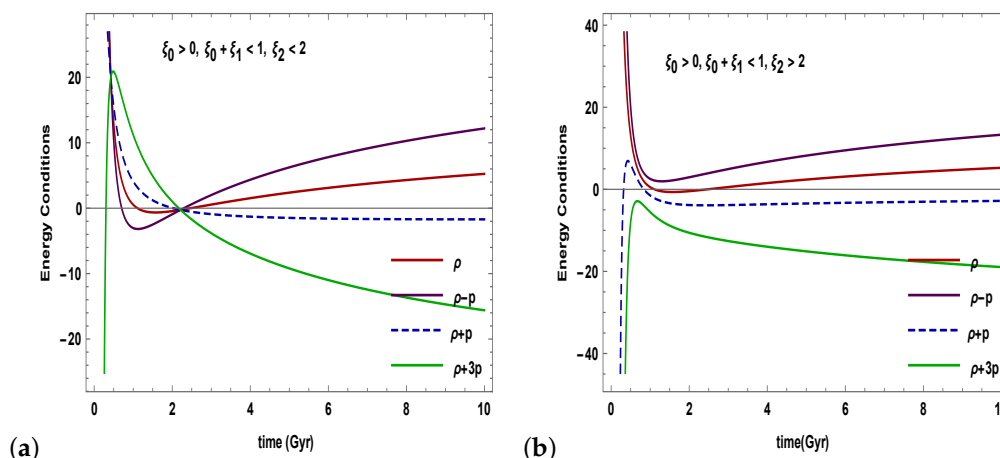


Figure 4. Cont.

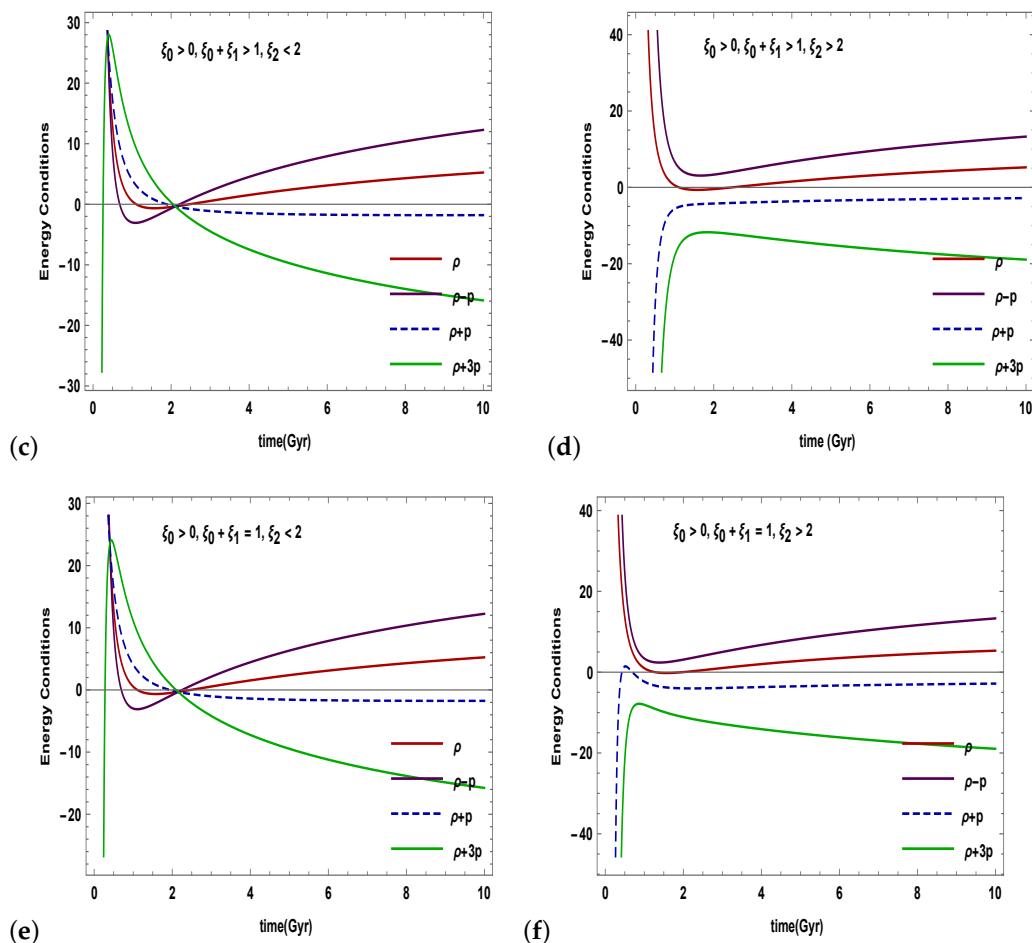


Figure 4. The variation of energy condition versus time t for various bulk viscosity coefficients.

6. $f(T, B)$ Tachyon Model

Here, we investigate the correspondence of $f(T, B)$ gravity with the tachyon scalar field. The tachyon model, which emerged from string theory, has been proposed to account for the DE scenario [103]. The fact that a rolling tachyon interpolates the EoS value between -1 and 0 is an intriguing feature. The greatest contender for inflation at high energy is the tachyon model, as well. There have been numerous attempts to create trustworthy cosmological models using various self-interacting potentials, as noted in [104]. According to reference [103], this scalar field has the following energy and pressure:

$$\rho_T = \frac{v(\phi)}{\sqrt{1-\dot{\phi}^2}} \quad p_T = -v(\phi)\sqrt{1-\dot{\phi}^2} \tag{31}$$

Now, solving Equations (28) and (29), we have obtained the density of scalar field $\dot{\phi}^2$ and potential of $f(T, B)$ gravity as $V(\phi)$, leading to the EoS parameter as;

$$\omega_T = 1 - \dot{\phi}^2 \tag{32}$$

$$\begin{aligned}
 \phi^2 = 1 + & \left[\frac{\alpha^2 e^{2\alpha mt}}{18(e^{\alpha mt} - 1)^2} \left(-\frac{18\alpha e^{\alpha mt} (a(e^{\alpha mt} - 1)^2 + \alpha e^{\alpha mt} (b(e^{\alpha mt} - 1) + \alpha c(e^{\alpha mt} - m)))}{(e^{\alpha mt} - 1)^3} \right. \right. \\
 & + \frac{18\alpha^2 \beta e^{2\alpha mt}}{(e^{\alpha mt} - 1)^2} \\
 & + \frac{2\gamma m^2 e^{\alpha(-m)t} ((m - 6)e^{\alpha mt} + n)^2}{(3e^{\alpha mt} - m)^3} + \frac{\gamma m^2 e^{\alpha(-m)t} ((m - 6)e^{2\alpha mt} + 4(m - 3)e^{\alpha mt} + m)}{(m - 3e^{\alpha mt})^2} \\
 & + \frac{3m(\gamma + (12\alpha^2(\beta + 1) + \gamma)e^{2\alpha mt} - 2e^{\alpha mt}(\gamma + 2\alpha^2(\beta + 1)m))}{(e^{\alpha mt} - 1)^2(3e^{\alpha mt} - m)} \\
 & - \frac{9e^{\alpha mt}(\gamma + (6\alpha^2(2\beta + 1) + \gamma)e^{2\alpha mt} - 2e^{\alpha mt}(\gamma + \alpha^2(2\beta + 1)m))}{(e^{\alpha mt} - 1)^2(3e^{\alpha mt} - m)} \\
 & \left. \left. + 3\gamma \log \left(\frac{6\alpha^2 e^{\alpha mt} (3e^{\alpha mt} - m)}{(e^{\alpha mt} - 1)^2} \right) \right) \right] \tag{33}
 \end{aligned}$$

$$\begin{aligned}
 V(\phi) = & \frac{1}{2\sqrt{3}} \left(\left(\frac{1}{(e^{\alpha mt} - 1)^2(m - 3e^{\alpha mt})^2} (e^{3\alpha mt} (-18\gamma + \gamma m^2 - 12m(3\alpha^2(\beta + 1) + \gamma))) \right. \right. \\
 & + \frac{2\gamma m^2 e^{\alpha(-m)t} ((m - 6)e^{\alpha mt} + m)^2}{(3e^{\alpha mt} - m)^3} + \frac{18\alpha^2 \beta e^{2\alpha mt}}{(e^{\alpha mt} - 1)^2} \\
 & + \frac{\gamma m^2 e^{\alpha(-m)t} ((m - 6)e^{2\alpha mt} + 4(m - 3)e^{\alpha mt} + n)}{(m - 3e^{\alpha mt})^2} \\
 & + \frac{3m(\gamma + (12\alpha^2(\beta + 1) + \gamma)e^{2\alpha mt} - 2e^{\alpha mt}(\gamma + 2\alpha^2(\beta + 1)m))}{(e^{\alpha mt} - 1)^2(3e^{\alpha mt} - m)} + 3\gamma \log \left(\frac{6\alpha^2 e^{\alpha mt} (3e^{\alpha mt} - n)}{(e^{\alpha mt} - 1)^2} \right) \\
 & - \frac{9e^{\alpha mt}(\gamma + (6\alpha^2(2\beta + 1) + \gamma)e^{2\alpha mt} - 2e^{\alpha mt}(\gamma + \alpha^2(2\beta + 1)m))}{(e^{\alpha mt} - 1)^2(3e^{\alpha mt} - m)} \\
 & + \frac{18\alpha e^{\alpha mt} (a(e^{\alpha mt} - 1)^2 + \alpha e^{\alpha mt} (b(e^{\alpha mt} - 1) + \alpha c(e^{\alpha mt} - m)))}{(e^{\alpha mt} - 1)^3} \\
 & - (2\gamma m^2 + 3e^{2\alpha mt} (3\gamma + 2\alpha^2(\beta + 1)m^2 + 8\gamma m) + 9(6\alpha^2(\beta + 1) + \gamma)e^{4\alpha mt} - 3\gamma(m + 4)m e^{\alpha mt} \\
 & \left. \left. - \gamma \left(-(e^{\alpha mt} - 1)^2 \right) (m - 3e^{\alpha mt})^2 \log \left(\frac{6\alpha^2 e^{\alpha mt} (3e^{\alpha mt} - m)}{(e^{\alpha mt} - 1)^2} \right) \right) \right)^{1/2} \tag{34}
 \end{aligned}$$

In Figure 5, the evolution of the tachyon scalar field as a function of time indicates that the tachyon scalar field ϕ^2 increases with time and finally approaches a positive value (see Figure 5a). However, the kinetic energy $V(\phi)$ of the tachyon potential decreases and will vanish in the future [105] (Figure 5b).

We can also notice the potential decreases initially, but increases as the scalar field increases (Figure 5c). The corresponding potential function expresses decreasing but positive behavior with respect to t . Its decreasing behavior from maxima gives inverse proportionality to the scalar field for the later times. This type of behavior corresponds to scaling solutions in the brane-world cosmology.

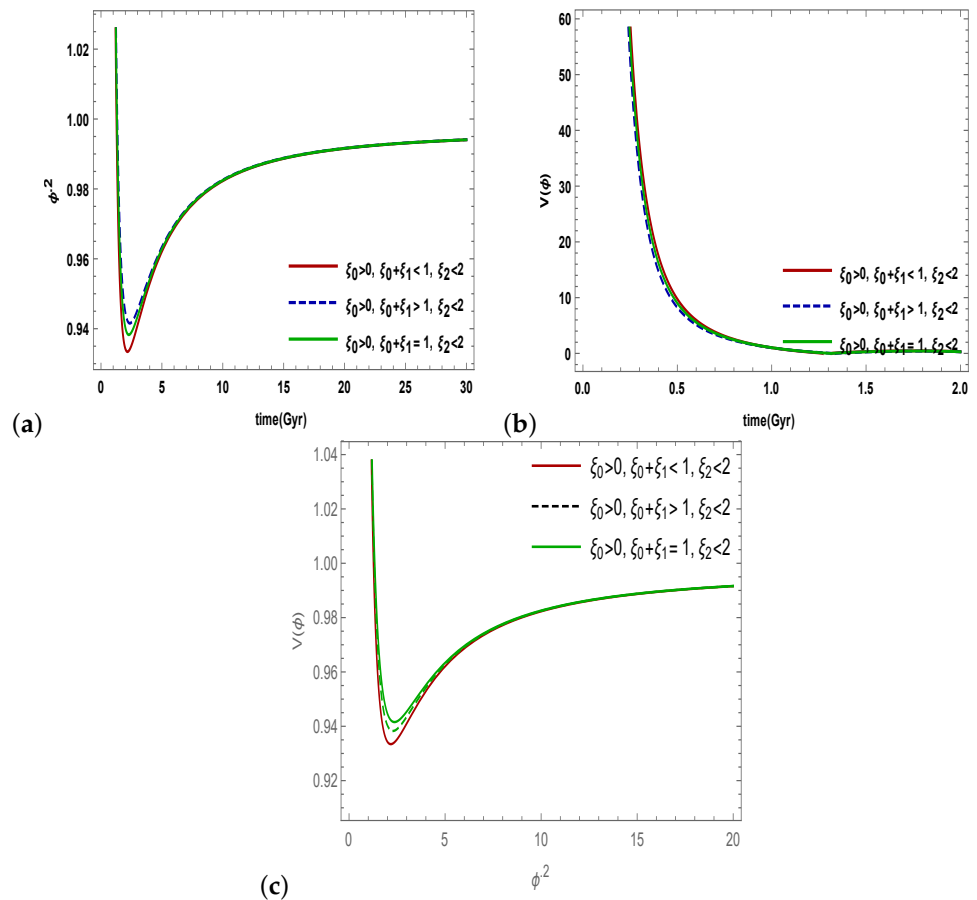


Figure 5. Correspondence of tachyon scalar field and potential versus t for various values of bulk viscosity coefficients.

7. Conclusions

Recently, teleparallel theories of gravity and their extensions have drawn a lot of attention in an effort to address a variety of cosmological issues. These theories are situated in a globally flat torsionally supported manifold. As we know, the GR has a teleparallel equivalent representation (TEGR) based on torsion (and tetrads) rather than curvature (and metric). From this perspective, many modified teleparallel ideas have been advanced. By changing the torsion scalar T in the action, the first one also referred to as $f(T)$ gravity naturally generalizes the TEGR action. This approach is comparable to $f(R)$ gravity's metric equivalent. These two concepts have provided a very accurate description of the cosmic behavior of the cosmos. In order to unify both $f(R)$ and $f(T)$ gravity and to investigate the relations between these theories, a modified teleparallel theory of gravity called the $f(T, B)$ theory was devised, which, within some constraints, can recover either $f(T)$ or $f(R)$ gravity.

In this work, we have obtained the cosmological analysis for the teleparallel $f(T, B)$ theory of gravity for flat FRW space-time. To find the exact solution of the field equations, we considered the particular form of $f(T, B) = \gamma \log(B) + \beta T$, which is proposed in [65]. We have estimated cosmological parameters and investigated the model's physical and geometrical behavior.

This paper also explores the behavior of viscosity by considering dust matter in the background of $f(T, B)$ gravity. We have assumed the logarithm well-known $f(T, B)$ models to evaluate the cosmological parameters. Using 46 OHD points, we have calculated the cosmological parameter values of the resultant models in the present paper.

The main findings of our paper are as follows:

- One-dimensional marginalized distribution and two-dimensional contour plots and error bar plots of the Hubble data set are shown in Figures 1 and 2.
- Figure 3 shows the effective equation of state parameter involving the bulk viscous pressure $\omega_{eff} = \frac{p_T + \Pi}{\rho_m + \rho_T}$. The evolutionary trajectory of the EoS parameter exhibits quintom-like behavior (transition from phantom to quintessence and evolution of the LCDM limit) for the limiting conditions of the viscosity parameter $\xi_0 > 0$ shown in (Figure 3a).
- We have seen that the viscous EoS parameter achieves a phantom-like universe for a particular choice of for $\xi_0 < 0$ shown in (Figure 3b). Thus, the viscous EoS parameter represents a DE-dominated universe for all the models depending upon model parameters. This behavior is compatible with the $f(TB)$ gravity model.
- Figure 4 shows the temporal evolution of the energy conditions. Keep in mind that to serve the late-time acceleration of the universe, the SEC has to violate. The SEC is the most discussed of all the energy conditions. According to recent findings from the speeding universe, the SEC must be violated on a cosmological scale. In our derived model, NEC, WEC, and DEC satisfy the criteria established from the Raychaudhuri equations. However, SEC is violated. As a consequence, our model is accurate and its solutions are physically feasible.
- Figure 5 depicts the correspondence between the scalar field and the $f(T, B)$ gravity model. We have noticed that the scalar field ϕ increases and potential decreases as time increases. The corresponding potential function exhibits a positive but decreasing relationship with time. Later, the scalar field exhibits inverse proportionality to its decreasing behavior from its maximum. In the brane-world cosmology, this kind of behavior corresponds to scaling solutions.

Given the findings discussed above, we can anticipate that an extension in the form of $f(T, B)$ gravity could lead to exciting situations where we can consider how torsion and boundary terms mix with astrophysical evidence to shed light on the study of the late-time accelerating universe.

Author Contributions: The authors contributed equally in this work. All authors have read and agreed to the published version of the manuscript.

Funding: This research received no external funding.

Data Availability Statement: Not applicable.

Acknowledgments: Anirudh Pradhan and Archana Dixit thank the IUCAA, Pune, India for providing facilities under associateship programs. The authors also express their gratitude to the reviewers for valuable comments and suggestions that improved the paper in the present form.

Conflicts of Interest: The authors declare no conflict of interest.

References

1. Perlmutter, S.; Aldering, G.; Goldhaber, G.; Knop, R.A.; Nugent, P.; Castro, P.G.; Deustua, S.; Fabbro, S.; Goobar, A.; Groom, D.E.; et al. Measurements of Ω and Λ from 42 high-redshift supernovae. *Astrophys. J.* **1999**, *517*, 565–586. [[CrossRef](#)]
2. Riess, A.G.; Filippenko, A.V.; Challis, P.; Clocchiatti, A.; Diercks, A.; Garnavich, P.M.; Gilliland, R.L.; Hogan, C.J.; Jha, S.; Kirshner, R.P.; et al. Observational evidence from supernovae for an accelerating universe and a cosmological constant. *Astron. J.* **1998**, *116*, 1009–1038. [[CrossRef](#)]
3. Ade, P.A.; Aghanim, N.; Ahmed, Z.; Aikin, R.W.; Alexander, K.D.; Arnaud, M.; Aumont, J.; Baccigalupi, C.; Banday, A.J.; Barkats, D.; et al. Joint analysis of BICEP2/Keck Array and Planck data. *Phys. Rev. Lett.* **2015**, *114*, 101301. [[CrossRef](#)] [[PubMed](#)]
4. Ade, P.A.; Aghanim, N.; Arnaud, M.; Ashdown, M.; Aumont, J.; Baccigalupi, C.; Banday, A.J.; Barreiro, R.B.; Bartlett, J.G.; Bartolo, N.; et al. Planck 2015 results XIII. Cosmological parameters. *Astron. Astrophys.* **2016**, *594*, A13.
5. Clifton, T.; Ferreira, P.G.; Padilla, A.; Skordis, C. Modified gravity and cosmology. *Phys. Rep.* **2012**, *513*, 1–189. [[CrossRef](#)]
6. Nojiri, S.; Odintsov, S.D. Introduction to modified gravity and gravitational alternative for dark energy. *Int. J. Geom. Methods Mod.* **2007**, *4*, 115. [[CrossRef](#)]
7. Starobinsky, A.A. A new type of isotropic cosmological models without singularity. *Phys. Lett. B* **1980**, *91*, 99. [[CrossRef](#)]
8. Nojiri, S.; Odintsov, S.D. Unified cosmic history in modified gravity: From $f(R)$ theory to Lorentz non-invariant models. *Phys. Rep.* **2011**, *505*, 59. [[CrossRef](#)]

9. Glavan, D.; Lin, C. Einstein-Gauss-Bonnet gravity in four-dimensional spacetime. *Phys. Rev. Lett.* **2020**, *124*, 081301. [[CrossRef](#)]
10. Harko, T.; Lobo, F.S.N.; Nojiri, S.; Odintsov, S.D. $f(R, T)$ gravity. *Phys. Rev. D* **2011**, *84*, 024020. [[CrossRef](#)]
11. Odintsov, S.D.; Oikonomou, V.K.; Fronimos, F.P. Rectifying Einstein-Gauss-Bonnet inflation in view of GW170817. *Nucl. Phys. B* **115135**, *958*, 115135. [[CrossRef](#)]
12. Anagnostopoulos, F.K.; Basilakos, S.; Saridakis, E.N. Bayesian analysis of $f(T)$ gravity using $f\sigma 8$ data. *Phys. Rev. D* **2019**, *100*, 083517. [[CrossRef](#)]
13. Unzicker, A.; Case, T.; Translation of Einstein's attempt of a unified field theory with teleparallelism. *arXiv* **2005**, arXiv:physics/0503046.
14. Hayashi, K.; Shirafuji, T.; New general relativity. *Phys. Rev. D* **1979**, *19*, 3524. [[CrossRef](#)]
15. Pradhan, A.; Dixit, A. Anisotropic MHRDE model in BD theory of gravitation. *Int. J. Geom. Methods Mod.* **2019**, *16*, 1950185. [[CrossRef](#)]
16. Dixit, A.; Pradhan, A. Stability, dark energy parameterization and swampland aspect of Bianchi type-VIIh cosmological models with $f(R, T)$ -gravity. *Int. J. Geom. Methods Mod.* **2020**, *17*, 2050213. [[CrossRef](#)]
17. Samanta, G. C.; Godani, N. Physical parameters for stable $f(R)$ models. *Indian J. Phys.* **2021**, *94*, 1303. [[CrossRef](#)]
18. Pradhan, A.; Maurya, D.C.; Dixit, A. Dark energy nature of viscous universe in $f(R)$ -gravity with observational constraints. *Int. J. Geom. Methods Mod. Phys.* **2021**, *18*, 2150124. [[CrossRef](#)]
19. Ferraro, R.; Fiorini, F. Modified teleparallel gravity: Inflation without an inflaton. *Phys. Rev. D* **2007**, *75*, 084031. [[CrossRef](#)]
20. Bamba, K.; Geng, C.Q.; Lee, C.C.; Luo, L.W. Equation of state for dark energy in $f(T)$ gravity. *J. Cosmol. Astropart. Phys.* **2011**, *01*, 021. [[CrossRef](#)]
21. Golovnev, A.; Guzman, M.-J. Approaches to spherically symmetric solutions in $f(T)$ gravity. *Universe* **2021**, *7*, 121. [[CrossRef](#)]
22. Pfeifer, C.; Schuster, S. Static spherically symmetric black holes in weak $f(T)$ - gravity. *Universe* **2021**, *7*, 153. [[CrossRef](#)]
23. Bahamonde, S.; Capozziello, S. Noether symmetry approach in $f(T, B)$ teleparallel cosmology. *Eur. Phys. J. C* **2017**, *77*, 1–10. [[CrossRef](#)] [[PubMed](#)]
24. Escamilla, C.R.; Said, J.L. Cosmological viable models in $f(T, B)$ theory as solutions to the H_0 tension. *Class Quantum Gravit.* **2020**, *37*, 165002. [[CrossRef](#)]
25. Shekh, S.H.; Chirde, V.R.; Sahoo, P.K. Energy conditions of the $f(T, B)$ gravity dark energy model with the validity of thermodynamics. *Comm.Theor. Phys.* **2020**, *22*, 085402. [[CrossRef](#)]
26. Godani, N. Locally rotationally symmetric Bianchi type-II cosmological model in $f(R, T)$ gravity. *Ind. J. Phys.* **2019**, *93*, 951. [[CrossRef](#)]
27. Pradhan, A.; Garg, P.; Dixit, A. FRW cosmological models with cosmological constant in $f(R, T)$ theory of gravity. *Can. J. Phys.* **2021**, *99*, 741. [[CrossRef](#)]
28. Tiwari, R.K.; Beesham, A.; Mishra, S.; Dubey, V. Anisotropic cosmological model in a modified theory of gravitation. *Universe* **2021**, *7*, 226. [[CrossRef](#)]
29. Bhardwaj, V.K.; Pradhan, A. Evaluation of cosmological models in $f(R, T)$ gravity in different dark energy scenario. *New Astron.* **2022**, *91*, 101675. [[CrossRef](#)]
30. Tangphati, T.; Hansraj, S.; Banerjee, A.; Pradhan, A. Quark stars in $f(R, T)$ gravity with an interacting quark equation of state. *Phys. Dark Univ.* **2022**, *35*, 100990. [[CrossRef](#)]
31. Pretel, J.M.Z.; Tangphati, T.; Banerjee, A.; Pradhan, A. Charged quark stars in $f(R, T)$ gravity. *Chin. Phys. C* **2022**, *46*, 115103. [[CrossRef](#)]
32. Pradhan, A.; Dixit, A. The model of the transit cosmology along with observational constraints in $f(Q, T)$ gravity. *Int. J. Geom. Methods Mod.* **2021**, *18*, 2150159. [[CrossRef](#)]
33. Godani, N.; Samanta, G.C. FRW cosmology in $f(Q, T)$ gravity. *Int. J. Geom. Methods Mod.* **2021**, *18*, 2150134. [[CrossRef](#)]
34. Nojiri, S.; Odintsov, S.D.; Tretyakov, P.V. From inflation to dark energy in the non-minimal modified gravity. *Prog. Theor. Phys. Suppl.* **2008**, *172*, 81. [[CrossRef](#)]
35. Elizalde, E.; Myrzakulov, R.; Obukhov, V.V.; Saez-Gomez, D. Λ CDM epoch reconstruction from $F(R, G)$ and modified Gauss-Bonnet gravities. *Class. Quantum Gravity* **2010**, *27*, 095007. [[CrossRef](#)]
36. Banerjee, A.; Pradhan, A.; Tangphati, T.; Rahaman, F. Wormhole geometry in $f(Q)$ gravity and the energy conditions. *Eur. Phys. J. C* **2021**, *81*, 10131. [[CrossRef](#)]
37. Gupta, S.; Dixit, A.; Pradhan, A. Tsallis holographic dark energy scenario in viscous $F(Q)$ gravity and techyan field. *Int. J. Geom. Methods Mod.* **2022**. [[CrossRef](#)]
38. Pradhan, A.; Dixit, A.; Maurya, D.C. Quintessence behaviour of an anisotropic bulk viscous cosmological model in modified $f(Q)$ gravity. *arXiv* **2022**, arXiv:2210.13730.
39. Iosifidis, D.; Myrzakulov, N.; Myrzakulov, R. Metric-affine version of Myrzakulov $F(R, T, Q, \tau)$ gravity and cosmological applications. *Universe* **2021**, *7*, 262. [[CrossRef](#)]
40. Mardan, S.A.; Amjad, A.; Noureen, I. Frameworks of generalized anisotropic conformally flat polytropes in $f(R)$ gravity. *Eur. Phys. J. C* **2022**, *82*, 794. [[CrossRef](#)]
41. Noureen, I.; Arshad, N.; Mardan, S.A. Development of local density perturbation scheme in $f(R)$ gravity to identify cracking points. *Eur. Phys. J. C* **2022**, *82*, 621. [[CrossRef](#)]
42. Noureen, I.; Haq, U.; Mardan, S.A. Impact of $f(R, T)$ gravity in evolution of charged viscous fluids. *Int. J. Mod. Phys. D* **2021**, *30*, 2150027. [[CrossRef](#)]

43. Franco, G.A.; E-Rivera, C.; Levi Said, J. Stability analysis for cosmological models in $f(T, B)$ gravity. *Eur. Phys. J. C* **2020**, *80*, 1. [[CrossRef](#)]
44. Paliathanasis, A. Anisotropic spacetimes in $f(T, B)$ theory I: Bianchi I universe. *Eur. Phys. J. C* **2022**, *137*, 1. [[CrossRef](#)]
45. Shekh, S.H.; Moraes, H.R.S.; Sahoo, P.K. Physical acceptability of the Renyi, Tsallis and Sharma-Mittal holographic dark energy models in the $f(T, B)$ gravity under Hubble's cutoff. *Universe* **2021**, *7*, 67. [[CrossRef](#)]
46. Escamilla-Rivera, C.; Rave-franco, G.; Levi-Said, J. $f(T, B)$ cosmography for high redshifts. *Universe* **2021**, *7*, 441. [[CrossRef](#)]
47. Li, B.; Sotiriou, T.P.; Barrow, J.D. $f(T)$ gravity and local Lorentz invariance. *Phys. Rev. D* **2011**, *83*, 064035. [[CrossRef](#)]
48. Krssak, M.; Saridakis, E.N. The covariant formulation of $f(T)$ gravity. *Class. Quant. Grav.* **2016**, *33*, 115009. [[CrossRef](#)]
49. Paliathanasis, A. de Sitter and Scaling solutions in a higher-order modified teleparallel theory. *JCAP* **2017**, *1708*, 027. [[CrossRef](#)]
50. Karpathopoulos, L.; Basilakos, S.; Leon, G.; Paliathanasis, A.; Tsamparlis, M. Cartan symmetries and global dynamical systems analysis in a higher-order modified teleparallel theory. *Gen. Rel. Gravity* **2018**, *50*, 79. [[CrossRef](#)]
51. Caruana, M.; Farrugia, G.; Said, J.L. Cosmological bouncing solutions in $f(T, B)$ gravity. *Eur. Phys. J. C* **2020**, *80*, 1. [[CrossRef](#)]
52. Paliathanasis, A. Cosmological evolution and exact solutions in a fourth-order theory of gravity. *Phys. Rev. D* **2017**, *95*, 064062. [[CrossRef](#)]
53. Paliathanasis, A.; Leon, G. Cosmological evolution in $f(T, B)$ gravity. *Eur. Phys. J. Plus* **2021**, *136*, 1. [[CrossRef](#)]
54. Rave-Franco, G.A.; Escamilla-Rivera, C.; Said, J.L. Dynamical complexity of the teleparallel gravity cosmology. *Phys. Rev. D* **2021**, *103*, 084017. [[CrossRef](#)]
55. Paliathanasis, A.; Leon, G. $f(T, B)$ gravity in a Friedmann-Lemaître-Robertson-Walker universe with nonzero spatial curvature. *arXiv* **2022**, arXiv:2201.12189.
56. Paliathanasis, A. Minisuperspace Quantization of $f(T, B)$ Cosmology. *Universe* **2021**, *7*, 150. [[CrossRef](#)]
57. Najera, S.; Aguilar, A.; Rave-Franco, G.A.; Escamilla-Rivera, C.; Sussman, R.A. Inhomogeneous solutions in $f(T, B)$ gravity. *Int. J. Geom. Methods Mod. Phys.* **2022**, 2240003. [[CrossRef](#)]
58. Ren, J.; Meng, X.H. Cosmological model with viscosity media (dark fluid) described by an effective equation of state. *Phys. Lett. B* **2006**, *633*, 1. [[CrossRef](#)]
59. Tawfik, A.; Harko, T. Quark-hadron phase transitions in the viscous early universe. *Phys. Rev. D* **2012**, *85*, 084032. [[CrossRef](#)]
60. Sharif, M.; Rani, S. Viscous dark energy in $f(T)$ gravity. *Mod. Phys. Lett. A* **2013**, *28*, 1350118. [[CrossRef](#)]
61. Singh, C.P.; Kumar, P. Friedmann model with viscous cosmology in modified $f(R, T)$ gravity theory. *Eur. Phys. J. C* **2014**, *74*, 3070. [[CrossRef](#)]
62. Bahamonde, S.; Dialektopoulos, K.F.; Escamilla-Rivera, C.; Farrugia, G.; Gakis, V.; Hendry, M.; Hohmann, M.; Said, J.L.; Mifsud, J.; Di Valentino, E. Teleparallel gravity: From theory to cosmology. *arXiv* **2021**, arXiv:2106.13793.
63. Bahamonde, S.; Boehmer, C.G.; Wight, M. Modified teleparallel theories of gravity. *Phys. Rev. D* **2015**, *9*, 104042. [[CrossRef](#)]
64. Krssak, M.; Van Den Hoogen, R.J.; Pereira, J.G.; Bohmer, C.G.; Coley, A. Teleparallel theories of gravity: Illuminating a fully invariant approach. *Class. Quantum Grav.* **2019**, *36*, 183001. [[CrossRef](#)]
65. Bahamonde, S.; Zubair, M.; Abbas, G. Thermodynamics and cosmological reconstruction in $f(T, B)$ gravity. *Phys. Dark Univ.* **2018**, *19*, 78. [[CrossRef](#)]
66. Zimdahl, W. Bulk viscous cosmology. *Phys. Rev. D* **1996**, *53*, 5483. [[CrossRef](#)]
67. Eckart, C. The thermodynamics of irreversible processes. III. Relativistic theory of the simple fluid. *Phys. Rev.* **1940**, *58*, 919. [[CrossRef](#)]
68. Singh, J.P. A cosmological model with both deceleration and acceleration. *Astrophys. Space Sci.* **2008**, *318*, 103. [[CrossRef](#)]
69. Banerjee, N.; Das, S. Acceleration of the universe with a simple trigonometric potential. *Gen. Relativ. Gravit.* **2005**, *37*, 1695. [[CrossRef](#)]
70. Riess, A.G.; Strolger, L.G.; Tonry, J.; Casertano, S.; Ferguson, H.C.; Mobasher, B.; Challis, P.; Filippenko, A.V.; Jha, S.; Li, W.; et al. Type Ia supernova discoveries at $z \geq 1$ from the Hubble Space Telescope: Evidence for past deceleration and constraints on dark energy evolution. *Astrophys. J.* **2005**, *607*, 665. [[CrossRef](#)]
71. Tian, S. The relation between cosmological redshift and scale factor for photons. *Astrophys. J.* **2017**, *846*, 90. [[CrossRef](#)]
72. Wojtak, R.; Prada, F. Testing of mapping between redshift and cosmic scale factor. *Mon. Not. R. Astron. Soc.* **2016**, *458*, 3331. [[CrossRef](#)]
73. Gupta, R.P. SNe Ia redshift in a nonadiabatic universe. *Universe* **2018**, *4*, 104. [[CrossRef](#)]
74. Nagpal, R.; Pacif, S.K.J.; Singh, J.K.; Bamba, K.; Beesham, A. Analysis with observational constraints in Λ -cosmology in $f(R, T)$ gravity. *Eur. Phys. J. C* **2018**, *78*, 946. [[CrossRef](#)]
75. Goswami, G.K.; Pradhan, A.; Beesham, A. Friedmann-Robertson-Walker accelerating Universe with interactive dark energy. *Pramana* **2019**, *93*, 1. [[CrossRef](#)]
76. Yadav, A.K.; Alshehri, A.M.; Ahmad, N.; Goswami, G.K.; Kumar, M. Transitioning universe with hybrid scalar field in Bianchi I space-time. *Phys. Dark Univ.* **2021**, *31*, 100738. [[CrossRef](#)]
77. Macaulay, E.; Nichol, R.C.; Bacon, D.; Brout, D.; Davis, T.M.; Zhang, B.; Bassett, B.A.; Scolnic, D.; Möller, A.; D'Andrea, C.B.; et al. First cosmological results using Type Ia supernovae from the dark energy survey: Measurement of the Hubble constant. *Mon. Not. R. Astron. Soc.* **2019**, *486*, 2184–2196. [[CrossRef](#)]
78. Moresco, M.; Pozzetti, L.; Cimatti, A.; Jimenez, R.; Maraston, C.; Verde, L.; Thomas, D.; Citro, A.; Tojeiro, R.; Wilkinson, D. A 6% measurement of the Hubble parameter at $z \sim 0.45$: Direct evidence of the epoch of cosmic re-acceleration. *J. Cosmol. Astropart. Phys.* **2016**, *2016*, 014. [[CrossRef](#)]

79. Zhang, C.; Zhang, H.; Yuan, S.; Liu, S.; Zhang, T.J.; Sun, Y.C. Four new observational $H(z)$ data from luminous red galaxies in the Sloan Digital Sky Survey data release seven. *Res. Astron. Astrophys.* **2014**, *14*, 1221. [[CrossRef](#)]
80. Stern, D.; Jimenez, R.; Verde, L.; Kamionkowski, M.; Stanford, S.A. Cosmic chronometers: Constraining the equation of state of dark energy I: $H(z)$ measurements. *J. Cosmol. Astropart. Phys.* **2010**, *2010*, 008. [[CrossRef](#)]
81. Simon, J.; Verde, L.; Jimenez, R. Constraints on the redshift dependence of the dark energy potential. *Phys. Rev. D* **2005**, *71*, 123001. [[CrossRef](#)]
82. Alam, S.; Ata, M.; Bailey, S.; Beutler, F.; Bizyaev, D.; Blazek, J.A.; Bolton, A.S.; Brownstein, J.R.; Burden, A.; Chuang, C.H.; et al. The clustering of galaxies in the completed SDSS-III Baryon Oscillation Spectroscopic Survey: Cosmological analysis of the DR12 galaxy sample. *Mon. Not. R. Astron. Soc.* **2016**, *470*, 2617–2652. [[CrossRef](#)]
83. Anderson, L.; Aubourg, E.; Bailey, S.; Beutler, F.; Bhardwaj, V.; Blanton, M.; Bolton, A.S.; Brinkmann, J.; Brownstein, J.R.; Burden, A.; et al. The clustering of galaxies in the SDSS-III Baryon Oscillation Spectroscopic Survey: Baryon acoustic oscillations in the Data Releases 10 and 11 Galaxy samples. *Mon. Not. R. Astron. Soc.* **2014**, *441*, 24–62. [[CrossRef](#)]
84. Moresco, M.; Cimatti, A.; Jimenez, R.; Pozzetti, L.; Zamorani, G.; Bolzonella, M.; Dunlop, J.; Lamareille, F.; Mignoli, M.; Pearce, H.; et al. Improved constraints on the expansion rate of the Universe up to $z \sim 1.1$ from the spectroscopic evolution of cosmic chronometers. *J. Cosmol. Astropart. Phys.* **2012**, *2012*, 006. [[CrossRef](#)]
85. Blake, C.; Brough, S.; Colless, M.; Contreras, C.; Couch, W.; Croom, S.; Croton, D.; Davis, T.M.; Drinkwater, M.J.; Forster, K.; et al. The Wiggle Z Dark Energy Survey: Joint measurements of the expansion and growth history at $z < 1$. *Mon. Not. R. Astron. Soc.* **2012**, *425*, 405–414.
86. Gaztanaga, E.; Cabre, A.; Hui, L. Clustering of luminous red galaxies IV. Baryon acoustic peak in the line-of-sight direction and a direct measurement of $H(z)$. *Mon. Not. R. Astron. Soc.* **2009**, *399*, 1663–1680. [[CrossRef](#)]
87. Chuang, D.H.; Wang, Y. Modelling the anisotropic two-point galaxy correlation function on small scales and single-probe measurements of $H(z)$, $DA(z)$ and $f(z)$ from the Sloan Digital Sky Survey DR7 luminous red galaxies. *Mon. Not. R. Astron. Soc.* **2013**, *435*, 255. [[CrossRef](#)]
88. Moresco, M. Raising the bar: New constraints on the Hubble parameter with cosmic chronometers at $z \sim 2$. *Mon. Not. R. Astron. Soc.* **2015**, *450*, L16. [[CrossRef](#)]
89. Delubac, T.; Rich, J.; Bailey, S.; Font-Ribera, A.; Kirkby, D.; Le Goff, J.M.; Pieri, M.M.; Slosar, A.; Aubourg, E.; Bautista, J.E.; et al. Baryon acoustic oscillations in the Ly α forest of BOSS quasars. *Astron Astrophys.* **2013**, *552*, A96.
90. Delubac, T.; Bautista, J.E.; Rich, J.; Kirkby, D.; Bailey, S.; Font-Ribera, A.; Slosar, A.; Lee, K.G.; Pieri, M.M.; Hamilton, J.C.; et al. Baryon acoustic oscillations in the Ly α forest of BOSS DR11 quasars. *Astron Astrophys.* **2015**, *584*, A59. [[CrossRef](#)]
91. Ratsimbazafy, A.L.; Loubser, S.I.; Crawford, S.M.; Cress, C.M.; Bassett, B.A.; Nichol, R.C.; Vaisanen, P. Age-dating luminous red galaxies observed with the Southern African Large Telescope. *Mon. Not. R. Astron. Soc.* **2017**, *467*, 3239–3254. [[CrossRef](#)]
92. Font-Ribera, A.; Kirkby, D.; Miralda-Escude, J.; Ross, N.P.; Slosar, A.; Rich, J.; Aubourg, E.; Bailey, S.; Bhardwaj, V.; Bautista, J.; et al. Quasar-Lyman α forest cross-correlation from BOSS DR11: Baryon Acoustic Oscillations. *J. Cosmol. Astropart. Phys.* **2014**, *2014(05)*, 027. [[CrossRef](#)]
93. Hu, M.G.; Meng, X.H. Bulk viscous cosmology: Statefinder and entropy. *Phys. Lett. B* **2006**, *635*, 186. [[CrossRef](#)]
94. Meng, X.H.; Ren, J.; Hu, M.G. Friedmann cosmology with a generalized equation of state and bulk viscosity. *Commun. Theor. Phys.* **2007**, *47*, 379.
95. Mostafapoor, N.; Gron, O. Viscous Λ CDM universe models. *Astrophys. Space Sci.* **2011**, *333*, 357. [[CrossRef](#)]
96. Nojiri, S.; Odintsov, S.D. Future evolution and finite-time singularities in $f(R)$ gravity unifying inflation and cosmic acceleration. *Phys. Rev. D* **2008**, *78*, 046006. [[CrossRef](#)]
97. Solanki, R.; Pacif, J.K.S.; Parida, A.; Sahoo, P.K. Cosmic acceleration with bulk viscosity in modified $f(Q)$ gravity. *Phys. Dark Univ.* **2021**, *32*, 100820. [[CrossRef](#)]
98. Capozziello, S.; Nojiri, S.; Odintsov, S.D. The role of energy conditions in $f(R)$ cosmology. *Phys. Lett. B* **2018**, *781*, 99. [[CrossRef](#)]
99. Martin-Morunoa, P.; Visserb, M. Classical and semi-classical energy conditions. *arXiv* **2017**, arXiv:1702.05915.
100. Kontou, E.-A.; Sanders, K. Energy conditions in general relativity and quantum field theory. *Class. Quant. Grav.* **2020**, *37*, 193001. [[CrossRef](#)]
101. Santos, J.; Alcaniz, J.S.; Reboucas, M.J.; Carvalho, F.C. Energy conditions in $f(R, T)$ gravity. *Phys. Rev. D* **2007**, *76*, 083513. [[CrossRef](#)]
102. Carroll, S. Spacetime and Geometry. In *An Introduction to General Relativity*; Addison Wesley: Boston, MA, USA 2004.
103. Copeland, E.J.; Sami, M.; Tsujikawa, S. Dynamics of dark energy. *Int. J. Mod. Phys. D* **2006**, *15*, 1753. [[CrossRef](#)]
104. Mazumdar, A.; Panda, S.; Perez-Lorenzana, A. Assisted inflation via tachyon condensation. *Nucl. Phys. B* **2001**, *614*, 101. [[CrossRef](#)]
105. Salako, I.G.; Jawad, A.; Moradpour, H. Cosmological implications of scalar field dark energy models in $f(T, \tau)$ gravity. *Int. J. Geom. Methods Mod.* **2018**, *15*, 1850063. [[CrossRef](#)]